Proceedings World Geothermal Congress 2015
Melbourne, Australia, 19-25 April 2015

Determining Porosity and Permeability in Laminated Sandstones for Combined CO_2-Geothermal Reservoir Utilization

Saismruti Pradhan, Inga Moeck and Ben Rostron

Earth and Atmospheric Sciences, 1-26 Earth Sciences Building, Edmonton, University of Alberta, Alberta, Canada T6G 2E3

saismrut@ualberta.ca

Keywords: Thomas-Stieber method, sand fraction, porosity, laminated sandstones

ABSTRACT

The utilization of hydrothermal porous reservoirs for a combined use of CO_2 storage and heat extraction referred to as CO_2-Plume-Geothermal requires the identification of highly porous clean sandstone beds. Recognition of clean sandstones within thin shaly beds in heterogeneous sandstones and determination of their petrophysical properties from well log measurements is a challenging problem in reservoir evaluation. Direct log interpretation values do not represent the true layer properties, but rather an average of multiple beds, resulting in significant underestimation of the reservoir quality. An interpretation methodology called the Thomas-Stieber method has been discussed here in order to better characterize thin beds and maximize reservoir potential.This method allows the identification of clean sandstone sections in heterogeneous sandstones. Clean sandstones represent generally the high-porosity sections and thus good reservoirs. The quantification of such reservoirs may also help to delineate highly productive injection zones in laminated sandstone relevant for unconventional hydrocarbon, geothermal reservoirs and as well as CO_2 storage sites.

The porosity and permeability thus obtained can be used to estimate the heterogeneous migration pathways and distribution of injected CO_2. The same methods can also be used to identify pay zones in heterogeneous sandstones hosting hydrothermal resources. In order to estimate the productivity and injection of CO2 into these heterogeneous sandstones, it is essential to identify the volume and porosity of shale in the shaly sand units. Porosity in shaly sands varies with the amount and distribution of the clay minerals within the reservoir because the shale can be distributed through the sand in different ways, such as laminated, dispersed, structural, or any combination of these. With each of these configurations different gamma ray responses can be expected and this variable response can be used to determine the shale configuration. So, gamma ray logs and porosity logs are used to estimate the shale type and volume. Our results can thus help in the identification of target zones for CO_2 injection, their efficient measurement and also in estimating stored thermal fluid in sedimentary hydrothermal resources.

1. INTRODUCTION

Geothermal energy is increasingly playing an important role in addressing the need of the world in moving to cleaner renewable energy sources. Therefore, new technologies utilizing geothermal energy should be implemented rapidly. The Carbon Dioxide Plume Geothermal (CPG), (Randolph and Saar, 2011) is one such technology which could support the rapid expansion of geothermal energy utilization by extracting geothermal heat from naturally porous, permeable geologic formations. Unlike traditional geothermal energy, this technology utilizes stored supercritical carbon dioxide as its working fluid. However, a challenge for large-scale implementation of sequestration is its cost. Carbon capture utilization and storage (CCUS) could add 50% or more to the cost of fossil-fuel-based electricity generation. Therefore, the most viable initial opportunities for CPG will likely be at those sites where companies are already engaged in CCUS, or are planning to participate in CCUS activities. Aquistore is one such prospective carbon storage site where CPG technology could be utilized.

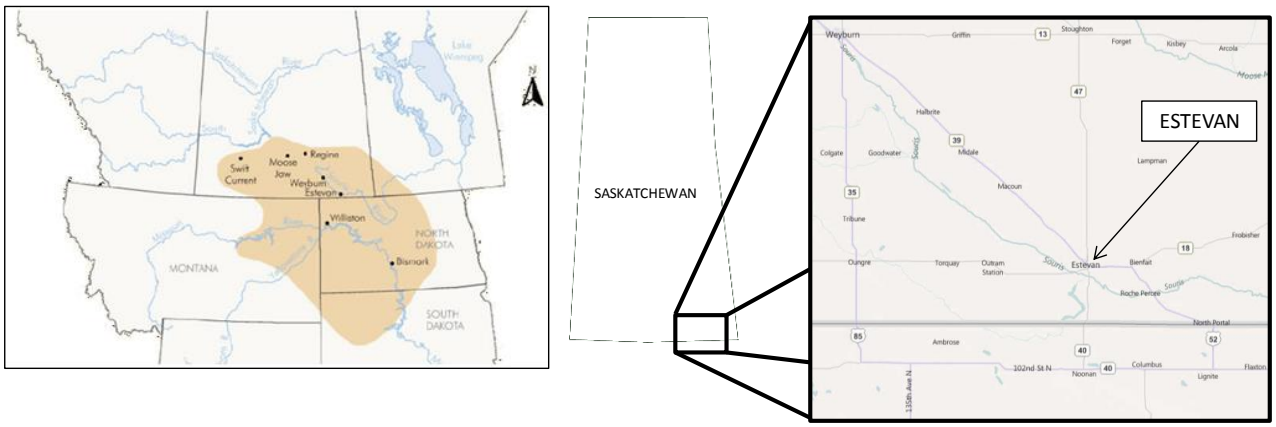

Figure 1: Location of Williston basin in the central North America. Aquistore is located in South East Saskatchewan, Canada near the community of Estevan

Aquistore is an independent research and monitoring project that stores liquid carbon dioxide in a deep brine sandstone water formation. It is located in in the Williston Basin in the south-eastern Saskatchewan, Canada (Fig.1). The geologic beds forming the

injection target are the Cambro-Ordovician flow unit within the Williston Basin that is comprised of the Deadwood Formation and Black Island member of the Winnipeg Formation (Whittakera and Worth, 2011). Aquistore has two wells, one injection well having total vertical depth of 3,396m and an observation well having total vertical depth of 3,400m. Having two recently drilled wells we have access to good quality well log data recorded by advanced logging tools and also available to us is a wide range of other useful data which makes it an ideal dataset to be used for our method.

The Deadwood and Winnipeg formations are the deepest sedimentary units in the Williston Basin with depth of more than 3,000m. The Deadwood Formation consists of sandstone and inter-bedded gray-green shale sequences (Kent and Christopher, 1994).These laminated shaly sand sequences could be bypassed if direct log interpretation techniques are applied in their evaluation. Direct log interpretation values will not give the true layer properties, but rather an average of multiple beds, resulting in significant underestimation of the reservoir quality (Pedersen and Nordahl, 1999). Therefore it is crucial to delineate and quantify shale occurrences in such laminated sandstone reservoirs. Our motive is to quantify the potential of such reservoirs by delineating highly productive intervals within the injection zones.

2. METHOD

The volume of dispersed shale and effective porosities of the laminar sand fraction are determined using a Thomas-Stieber (1975) volumetric approach. This shale volume can occur in various ways, such as dispersed shale, laminated shale, structural shale or their combination. The different shale configurations considered in the model are illustrated in Figure 2. As per the model, clean sand is sand consisting of sand grains and pore space with no clay, sand with dispersed shale is sand wherein all pores are filled with dispersed shale. In structural shale it is assumed that sand grains are replaced by shale "particles" without reducing original porosity, and in sand with dispersed and structural shale some sand grains are replaced by shale “particles” and all the pores are filled with dispersed shale. Lastly, in sand with laminated shale a part of sand is replaced with a shale lamination.

The basic assumptions of the method are that there are only two rock types; high porosity “clean” sand and low porosity “pure” shale. So the observed insitu properties are generated by mixing the two. Secondly, within the interval investigated, there is no change in shale type and the shale mixed in the sand is mineralogically the same as the “pure” shale sections above and below the sand. Thirdly, the gamma ray responds to the mass of the radioactive minerals in a formation and the shale fractions we wish to determine are a function of volume. Lastly, constant background radiation is assumed to be present in all measurements and the counting yields do not change as rock types are intermixed.

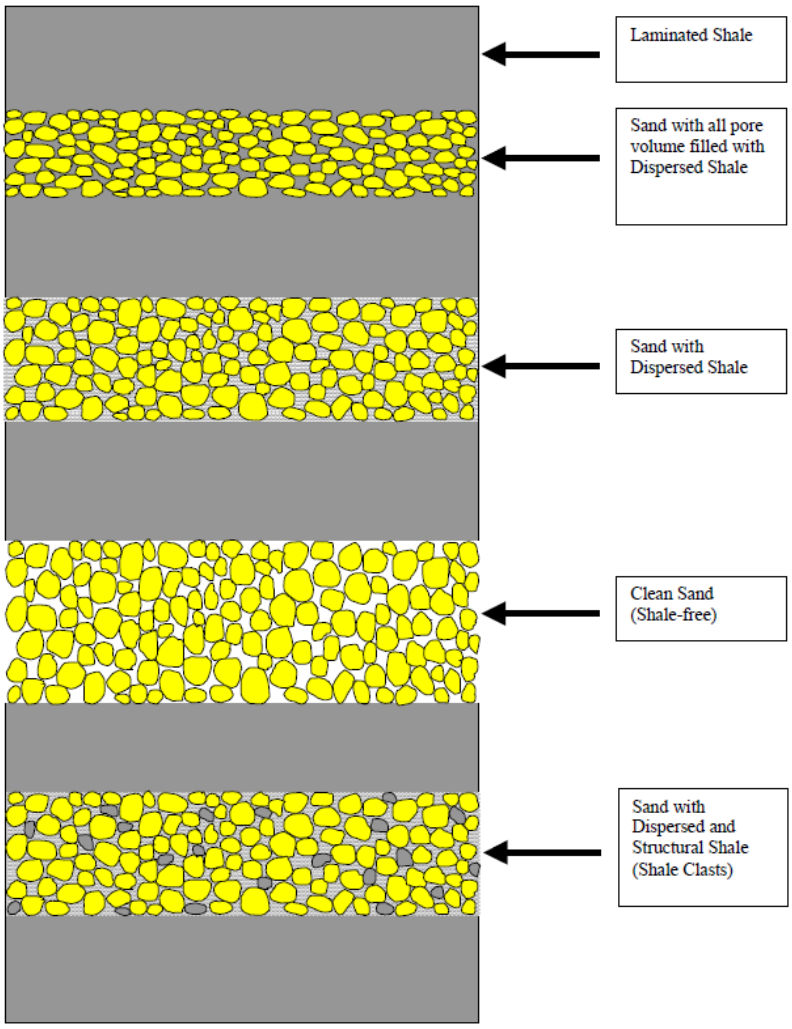

Figure 2: Sand and shale configuration considered in the model (Pedersen and Nordahl, 2000)

We use the gamma logs to estimate the shale volume and combining it with neutron porosity logs we estimate reservoir parameters such as sand fraction and sand porosity in the presence of different configuration of sand-shale sequences. This will not only help in the identification of suitable target zones for CO_2 injection, but also in efficient estimation of stored thermal fluid in hydrothermal reservoirs.

The shale volume is obtained using the following relation

$$I_{sh} = \frac{GR - GR_{clean}}{GR_{shale} - GR_{clean}} , \quad (1)$$

where, I_{sh} is the shale index, GR is the gamma ray log reading, GR_{clean} is the radioactivity of clean sand and GR_{shale} is the radioactivity of clean shales.

Dispersed shale only case: The sand fraction in this case determined from using following relation provided shale volume is greater than clean sand porosity

$$NG = 1 - X_{sh_d} , \quad (2)$$

where, NG is the sand fraction when the pore spaces are filled with dispersed shale only, X_{sh_d} is the volume of dispersed shale.

The porosity of the sand in the presence of dispersed shale is obtained using the following relationship

$$\emptyset_{sd} = \emptyset_{sd\_clean} - X_{sh_d}(1 - \emptyset_{sh}) \qquad \text{when } X_{sh_d} < \emptyset_{sd\_clean}, \quad (3)$$

$$\emptyset_{sd} = \emptyset_{sh} - NG\ \emptyset_{sh} \qquad \text{when } X_{sh_d} > \emptyset_{sd\_clean}, \quad (4)$$

where, $\emptyset_{sd}$is the porosity of sand with dispersed shale, $\emptyset_{sd\_clean}$ is the porosity of clean sand, $X_{sh_d}$is the shale volume and $\emptyset_{sh}$is the porosity of clean shale.

Laminated shale only case: The shale volume found above can be in the form of shale laminations within the sand body (Fig.2). The porosity in this case is found from the following relationship,

$$\emptyset_{SD\_Lam} = NG\ \emptyset_{SD_{Clean}} + (1 - NG)\emptyset_{sh} \quad (5)$$

Combination of laminated and dispersed case: The net to gross in this case is given by

$$NG_{dislam} = \frac{\frac{\emptyset_n - \emptyset_{sh}}{1 - \emptyset_{sh}} - \frac{NG}{\tau}}{\frac{\emptyset_{SD_{clean}} - \emptyset_{sh}}{1 - \emptyset_{sh}} - \frac{1}{\tau}} , \quad (6)$$

where, $\emptyset_n$is the porosity from log and$\tau = GR_{sh}/(GR_{sh} - GR_{clean})$

Porosity in the dispersed and lamination shale combination case is given by

$$\emptyset_{dislam} = \emptyset_{sd\_clean} - X_{sh_d}\emptyset_{sh} \quad (7)$$

3. DATASET

Good quality well log suite for the injection well is available. The gamma ray log, density log, neutron porosity log and resistivity log have been shown in Fig.3. The Aquistore project includes an injection and an observation well. The observation well is at a distance of 150m from the injection well. The geology is similar between the two wells. For the present work we have used the well logs from the injection well only. The gamma ray log data and neutron porosity data log from depth 3,150m-3,370m have been extracted from the dataset for the present purpose. This interval encounters the four injection zones, namely zone 1, zone 2, zone 3 and zone 4 as shown in the figure 3. The observed gamma ray log data is processed to estimate the shale fraction and estimate total porosity. Since the type of shale intercalations is not known in advance, we compute shale volume, sand fraction and sand porosity for dispersed, laminated and a combination of the two shale configurations. Porosities are validated using our method by comparing them with the porosities derived from cores.

The first step is to determine shale volume in the log interval from gamma ray intensities. For this purpose, the gamma ray intensity of clean sands and shales is required. Analysing the gamma ray intensities in the interval of interest show that maximum intensities do not exceed 260 API units and minimum intensities are not less than 10 API units. Since sands are characterised by low radioactivity and shales are characterized by high radioactivity, it has been assumed that gamma ray radioactivity of shales is 260 API units and clean sand intensity is 10 API units.

The neutron porosity values depend on presence of hydrogen which may not represent true porosity in all cases. Due to the increased depth the porosity values are quite low in this region. Thus, for the present analysis an effective porosity of 15% for clean sands and 3% for clean shales have been used. These are taken to be representative values for averaged clean sand and shales. If shale volume is less than clean shale clean sand porosity sand fraction is assumed to be 1. These parameters have been used in evaluating the sand fraction and porosity in the interval of interest. The gamma rays were examined and all negative values are eliminated since these are just null values and indicate no data. The same process is also applied to the neutron porosity logs.

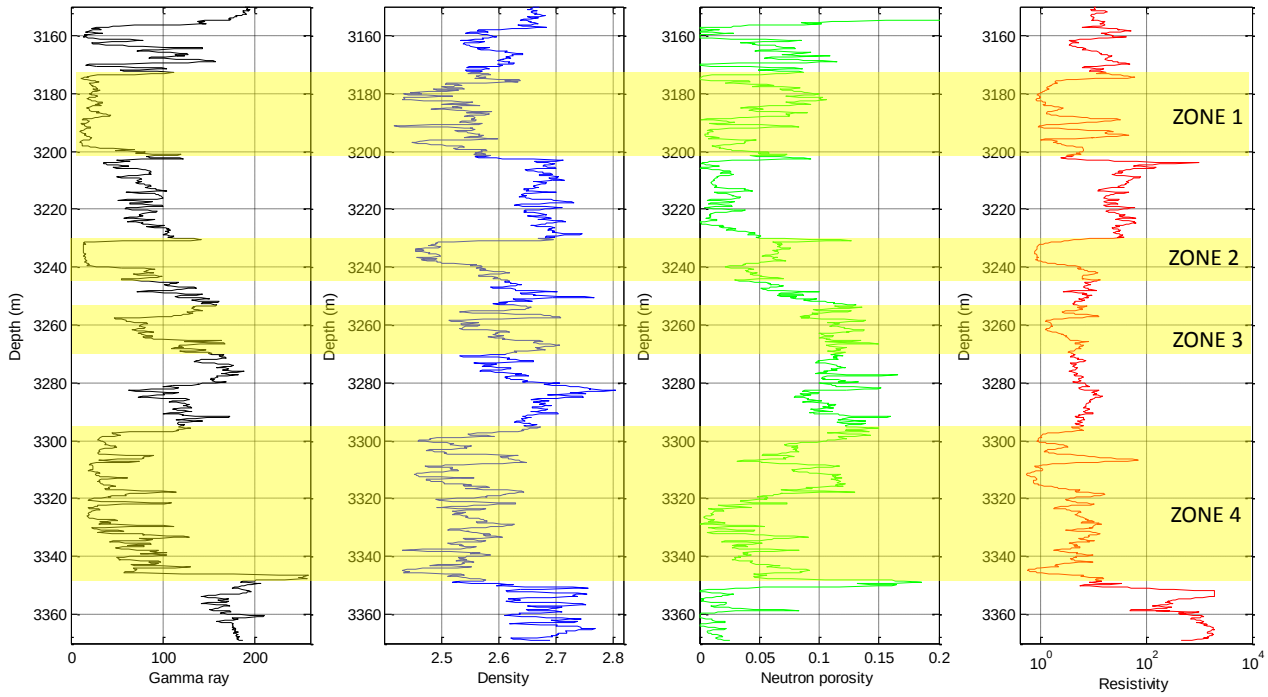

Figure 3: Well logs of the injection well. The four injection zones zone 1-4 are shown by the yellow shaded zones.

3. RESULTS AND DISCUSSIONS

In figure 4(a) the sand fraction values verses depth in the selected log interval for the dispersed shale case is shown. It has been assumed that when the shale volume is less than porosity of clean sand, sand fraction values are unity. The sand fraction values for the dispersed shales and laminated shales are the same. In some sections the sand fraction values also show portions where only clean sand is present. The laminated reservoirs with high shale fractions can be highly productive with reservoir quality equivalent to or maybe better than massive thick beds.

Fig. 4(b) shows the porosity values for the three types of shale distribution in the zone of interest. The porosity values for laminated shales are more than the dispersed shales and the combination of laminated and dispersed shale configuration tend to have the highest porosity. When shale is present in the form of laminations some part of sands may be free of shales and clean sand portions alternate with thin shale beds. It is also quite likely that at a given depth the shale is not present throughout the horizontal section but only in a part of it. In a more general case dispersed shale occurs as a combination with laminated shale. There cannot be any clean sand regions in this case. The porosity distribution with depth is intermediate between that of dispersed shale case and laminated shale case. The high porosity values for combination of dispersed and laminated shales observed here might be due to the high depth and compacted sandstones and require further analysis.

In case of structural shale, some sand grains are replaced by clay particles. The pore space is left unchanged. This is an ideal case and structural shale is assumed to be negligible here until further analysis. In practice some shale may escape into the pore spaces too. However, there may not be any substantial reduction in porosity in the presence of structural shale.

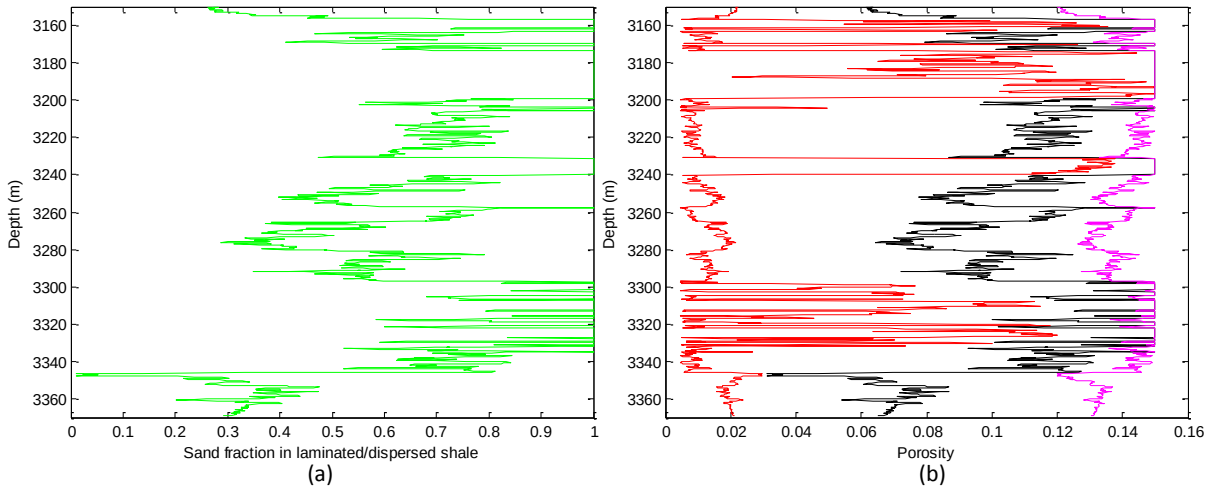

Figure 4: (a) Sand fraction in dispersed/laminated shale case. (b) Porosity obtained in case of dispersed shale (red curve), laminated shale (black) and in the combination of the two (magenta).

In figure 5 the extracted gamma ray log, bulk density and the computed porosities for dispersed case and laminated case is shown. The porosity of the sand beds in the injection zones have been affected the most by the presence of dispersed shales, especially in zone 3. In zone 4 the porosity seen in dispersed shale case is approximately 10% but in laminated shale case we have porosities upto 15% whereas the neutron gives us the lowest porosity.

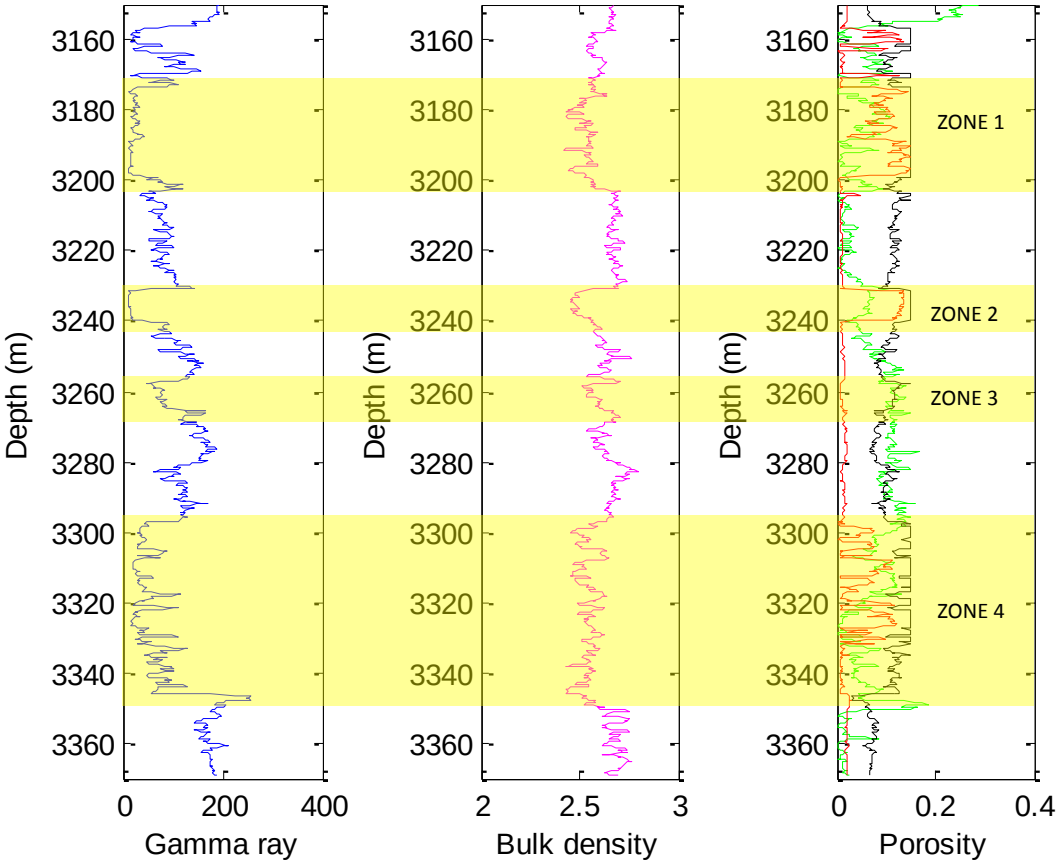

Figure 5: Gamma ray log, bulk density and a comparison of the neutron porosity log with the computed logs in the four zones of injection; green-neutron porosity log, red-dispersed shale case, black-laminated shale case.

Further, when we compare the neutron porosity log with our computed porosity values, we see higher values in our case. Figure 5 shows the comparison between the neutron porosity log and the obtained porosity logs in the dispersed and laminated shale case. We also see that in zones other than the injection zones the densities are quite high, which could indicate highly compacted sandstones or some lithology other than sandstone. This could be one such situation where the assumption of Thomas-Stieber is violated and lead to erroneous results.Thus, a certain amount of dispersed shale has a far more detrimental effect on the porosity of the sand than the same amount of shale concentrated into shale laminae between clean sand and further analysis is required to validate our results.

4. FUTURE WORK

Our next step would be to identify the thin shaly sand units within the target zones of Winnipeg and Deadwood sandstones from image logs and core data. However, core sample data are not available at the time of this study. Petrographical analysis of thin section samples from these shaly sands units of the injection zones would allow us to study the pore throat geometry and various mineralogy present. Depending on the type of configuration present our obtained results can be validated.

Removal of laminar shale conductivity and porosity effects reduces the shaly sand problem to a single dispersed shaly sand model to which the Waxman-Smits or equivalent equations can be applied (Mollison et al., 1999, Schonet al., and Page et al., 2001).

The partitioning of samples into laminated and dispersed clay dominated samples allows a formulation of specific NMR permeability models for each sample group. This would allow us to estimate the permeability of sand by using the Coates-Timur (Coates et al., 1991) equation,

$$k_{sd} = (\emptyset_{t_{sd}}/C)^n (BVI_{sd}/BVM_{sd})^b \quad (8)$$

where, k_{sd} is the permeability, $\emptyset_{t_{sd}}$ is the total porosity in sand, BVI_{sd} is the bulk volume irreducible, BVM_{sd} is the bulk volume moveable, C is constant, n is the saturation component and *b* is the bulk volume ratio exponent.

This is would be our next step after validating our results by comparing to core data.

5. CONCLUSIONS

Shale distribution is critical for correct reservoir characterization of low resistivity, low contrast laminated shaly sands. The Thomas-Stieber volumetric approach defined a relationship based on gamma ray log to determine laminar-dispersed or laminar sand fraction and total porosity. It should be noted that this methodology is based on a shale system, defined by differentiating laminar shale volume from total shale with the remainder being either structural or dispersed shale. Further, distinction of clay porosity end points or clay volume is undefined for this model. The key concept to this methodology lies in the removal of laminar shale effects on the sand fraction using a total porosity system. Though laminar shale does not occupy or alter the intergranular sand porosity, but does change the net to gross ratio. The computed sand fraction and porosity will provide greater authenticity after being compared to core data.

Estimating the net sand fraction and porosities in presence of dispersed, laminated or structural shales will aid us in evaluating the reservoir capacity efficiently for the injection zones. This will not only lead to estimating the heterogeneous migration pathways and distribution of injected CO_2 but may also help to delineate highly productive injection zones in laminated sandstone relevant for CO_2 storage and geothermal utilization.

ACKNOWLEDGEMENT

We would like to thank the Petroleum Technology Research Centre, Regina for granting permission to use the dataset and publish this work.

REFERENCES

Coates, G.R., Miller, M., Gillen, M., and Henderson, G.: The MRIL in Conoco 33-1--An Investigation of anew Magnetic Resonance Imaging Log," paper DD, 32nd Annual Logging Symposium Transactions: Society of Professional Well Log Analysts, (1991) p. 24.

Kent, D. M., and Christopher, J.E.: Geological history of the Williston Basin and Sweetgrass River Arch; in Geological Atlas of the Western Canada Sedimentary Basin, G.D. Mossop and I. Shetsen (comp.), Canadian Society of Petroleum Geologists and Alberta Research Council, (1994), pp.421-430.

Mollison, R., Scön, J., Fanini, O., Kriegshäuser, B., Meyer, H., and Gupta, P.; A model for hydrocarbon saturation estimation from an orthogonal tensor relationship in thinly laminated anisotropic reservoirs, paper OO, SPWLA 40th annual Logging Symposium Transactions (1999).

Pedersen, B.K. and Nordahl, K., Petrophysical evaluation of thin beds: a review of the Thomas-Stieber approach: Course 24034 Formation Evaluation 1, Semester report, (1999).

Randolph J. B., and Saar, M.: CPG: Geologically sequestered carbon dioxide as a geothermal heat mining fluid; applications and opportunities, 57th Annual Midwest Ground Water Conference, (2012).

Thomas, E. C., and Stieber, S.J.: The distribution of shale in sandstones and its effect upon porosity: 16th Annual Logging Symposium, SPWLA, Paper T (1975).

Whittaker, S., and Worth, K.: Aquistore: a fully integrated demonstration of the capture, transportation and geologic storage of CO_2 Energy Procedia 4, (2011) 5607–5614.